6 mechanotransduction

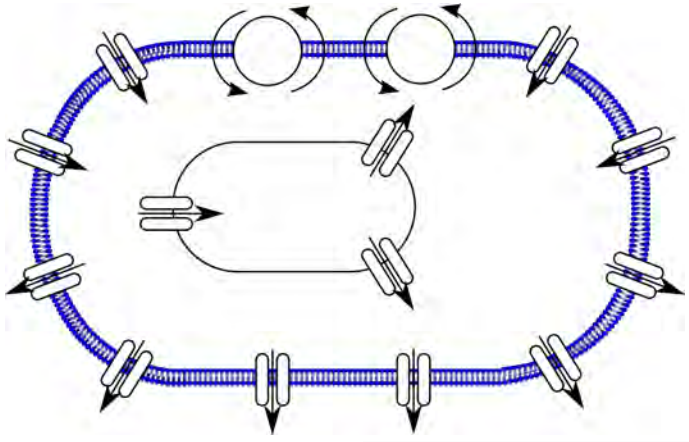

wong, goktepe, kuhl [2010]

downloadable layout file from coursework

ME239 FINAL PROJECT

Nicole Polizzi[1], Paul DelVecchio[2], and Mike Sorrentino[3]
Department of Mechanical Engineering, Stanford University
Stanford, California

Abstract. The abstract should summarize what you did and what you learned quantitatively. Summarize the important results for easy reference. Don't just write something along the lines of "This paper describes the design of X, outlines the fabrication and testing methods, and analyzes expected performance." Instead be specific about the main features of the design, results of your analysis, and summarize key features of how you would make and test it. The summary should be substantive but generally should not include figures or references. Your paper should summarize expected device performance quantitatively; describe methods, materials, challenges of your design. Formatting and content descriptions are provided here.

Background. In this section, discuss what you set out to do, your design requirements, and compare and contrast to prior work.

The Annual Poster Sessions for Stanford University's E240, Introduction to Micro and Nano Electromechanical Systems (M/NEMS), will be held on December 3 and 5, 2008, from 2:15 to 3:45 pm on the steps of the Durand building on Stanford University Campus. Papers for each project should be submitted electronically as PDF files by 5pm Tuesday, December 2. These papers will be printed and bound into "ENGR240 Class Proceedings" and distributed at the poster sessions.

- Affiliation: 11 points, regular;
- City, State: 12 points, regular;
- Text body: 10 points, regular; paragraphs without indent
- Figure captions: 10 points, *italic*;
- Table captions: 10 points, *italic*;
- References: 10 points, regular, numbered in [ ].

Analysis of Performance. In this section, you should quantify the expected performance of your design and how you will test it. Justify your assumptions and compare expected performance to existing devices. Graphs, tables, figures summarizing these data will convey this information succinctly.

downloadable sample project

THE PRIMARY CILIUM: A WELL-DESIGNED FLUID FLOW SENSOR

Bryan C. Petzold
Department of Mechanical Engineering, Stanford University
Stanford, California

The primary cilium is a highly specialized surface projection which extends from the apical surface of almost every vertebrate cell. After its initial discovery over 100 years ago, primary cilia were long overlooked and even purported by some to be extraneous genetic remnants from our evolutionary past. However, in the past decade, a wealth of evidence has begun to accumulate, indicating that cilia in various cell types act not only as mechanical and chemical sensors, but also play important roles in intracellular signaling and cell division[1]. Some have even suggested that cilia-related dysfunction may have an important role in modern human epidemics such as obesity, hypertension and diabetes[2]. One such link between cilia-related dysfunction and human disease that has been explored extensively involves the role of the primary cilia of renal epithelial cells as flow sensors. It is believed that a dysfunction in these cilia results in polycystic kidney disease (PKD), the most common inherited disease in the United States, with an estimated 600,000 current cases[3]. Numerous models have been proposed to explain the mechanotransduction mechanism which allows the primary cilia of renal epithelial cells to detect fluid flow, but many questions remain. Understanding the transduction mechanism and the features of the primary cilium which make it an ideal flow sensor will not only answer many interesting questions in biology and biomechanics, but could aid in the treatment of PKD and other diseases which are caused by cilia-related dysfunction.

INTRODUCTION TO THE PRIMARY CILIUM

The primary cilium is a long, cylindrical, microtubule-based structure which extends from the apical surface of most vertebrate cells, as shown in Figure 1. In general, cells only have a single primary cilium. Referred to as the axoneme, the main structural element of the primary cilium is a collection of nine circumferentially-arranged doublet microtubules encased by membrane continuous with the cell membrane[1]. These doublet microtubules extend from a structure known as a basal body within the cell, which links the base of the primary cilium to the cytoskeleton. The basal body consists of nine triplet microtubules, and two of the microtubules of each triplet form the axoneme of the primary cilium[1]. Further structural support is provided by the transitional fibers (also shields), which add stability to the complex via attachment to the cell membrane[1]. In conjunction with a terminal plate at the end of the basal body, these transitional fibers also act as a protein filter, only allowing certain proteins to enter and exit the cilium[1]. At the far end of the cilium, the axoneme becomes more variable, but is typically composed of nine single microtubules[1]. Although cilia are not isolated from the cell by a membrane, it seems reasonable to consider them to be organelles due to their unique structure, their extreme location past the cell periphery, and the selectivity to protein movement across their boundaries resulting from the transitional fibers and the terminal plate.

Depending on the species, primary cilia of renal epithelial cells typically vary between 2-20 μm in length *in vivo*[4]. However, lengths up to 30 μm have been observed *in vitro*[5]. In addition, studies involving mice renal epithelial cells measured primary cilia 2-3 μm long and 0.2 μm in diameter on average[1]. Since microtubules have an outer diameter of ~30 nm, this relatively small diameter indicates that nearly half the volume of a primary cilium is occupied by the microtubules alone[1].

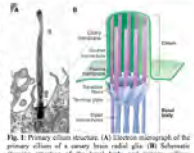

Fig. 1: Primary cilium structure. (A) Electron micrograph of the primary cilium of a ureter brain radial glia. (B) Schematic showing structure of the basal body and primary cilium. Adapted from Singla et al. (2006)[1].

downloadable grading criteria from coursework

Instructions for Judges
according to ASME / SBC conference review guidelines

The presentation format includes the **structure of the presentaiton and its composition**. In general, a presentation should be structured to include an introduction, method, analysis, results, a conclusion, and references. The introduction should define the problem, scope of the study, and a brief background of previous work. The method section also should be brief to leave the majority of the report body for results and discussion. The final paragraph should be a brief paragraph on inference or conclusions reached.

Technical merit should be judged on the completeness of what is reported. For scientific studies, the result should support the conclusions presented. The key is validation of the express conclusion with results and data. Unsubstantiated conclusions or results should receive minimum points. However, not all papers represent basic research. Some papers present the design of a hardware system or a new software development. Both require the development of tests and measurement procedures to validate the product.

After the scoring is complete, please indicate a final grade. Please provide a comment in the designated area that describes why you think this presentation suitable/not suitable. These comments will be collected and provide to the students for feedback.

Is not necessary for the judge to be an expert in the field represented by the paper to evaluate its technical merit using these criteria. Subjective rating of the paper's scientific contribution is not encouraged unless there is evidence that the conclusions are incorrect. A judge should feel free to consult colleagues who are experts in the field, if you are unsure about the correctness of the conclusions. Since presentations can vary from hardware designs to software technique, or simulations and modeling to basic research, each reviewer will have to use his/her own best judgement about the technical merit of the work that is presented.

Scoring & Evaluation System:

Please use the same scoring system as for the General Abstracts for each of the evaluation categories.

Score – Provide a ranking according to

Excellent	= 100
Very Good	= 90
Good	= 80
Marginal	= 60
Poor	= 50

Evaluation Categories

1. Structure of presentation
2. Technical merit
3. Style of presentation

Keep in mind the judges cannot be perfect, but will try to be consistent in scoring. There are multiple judges for each paper and each judge's scores will be normalized to compensate for individual variations.

download presentation schedule

	thursday, may 31, 2012
beth	measuring cell traction force
brittany	leukocyte activation
cesare	metastasis
dee ann	mechanics of cancer cells
elia,dong hyun,armen	cytoskeletal remodeling in endothelial cells
ernst	adipose cells
mengli	bone cells
ian	the role of podosomes in 3d cell migration
juna	skin cells
vaishnav	mechanics of cancer cells
	tuesday, june 5, 2012
alex	artificial red blood cells
brandon, matthew	vasculogenesis
corey, alex	red blood cells
elliot, pamon, ben	differentiation of mesenchymal cells
hwee juin	mechanotransduction in intestinal cells
kamil	directed stem cell differentiation
livia	dynamics of morphogenesis

mechanotransduction

the process of **converting physical forces into biochemical signals** and **integrating these signals into the cellular response** is referred to as mechnotransduction. to fully understand the molecular basis for mechanotransducion, we need to know how externally applied forces are transmitted into and throughout the cell. different techniques have been developed to **probe mechanotransduction** by mechanically stimulate cells to address the following questions.

What do we study in mechanotransduction? How do cells respond to mechanical forces? ○ How do mechanical forces lead to biochemical and molecular responses? ○ How can we strengthen bone? ○ How can we grow cartilage? ○ How can we strengthen muscle? ○ How can we improve cardiac contractility? ○ How can we engineer tissues for artificial organs? ○ How can we mimic the mechanical loading environment of cells in vitro? ○ What can we learn from mechanical stimulation of cells with precisely controlled forces?

mechanotransduction

the process of mechanotransduction can be divided into three steps

- **mechanoreception**
  detection of the stimulus and transmission of the signal from outside the cell to its inside
- **intracellular signal transduction**
  transduction of the stimulus to location in the cell where a molecular response can be generated
- **target activation**
  activation of proteins that cause alterations in cell behavior through a variety of different mechanisms

the cell membrane

all cellular components are contained within a cell membrane which is **extremely thin**, approximately 4-5nm, and **very flexible**. inside the cell membrane, most cells behave like a liquid as they consist of more than 50% of water. the cell membrane is **semi-permeable** allowing for a controlled exchange between intracellular and extracellular components and information.

mechanisms of transport through the membrane

- passive transport driven by gradients in concentration
- active transport that does require extra energy; it is regulated by ion channels, pumps, transporters, exchangers and receptors

the cell membrane

the cell membrane contains water-filled pores with diameters of about 0.8nm and **protein-fined pores called channels** which allow for the **controlled passage** of specific molecules, in particular Na^+, K^+, and Cl^-. the phospholipid bilayer acts as a barrier to the free flow of these ions maintaining a well-regulated **concentration difference** across the cell membrane which is referred to as **membrane potential**. this implies that the membrane can selectively separate charge.

$$\phi = \phi^{\text{int}} - \phi^{\text{ext}} \qquad \text{... membrane potential}$$

virtually all cells are **negatively charged**, i.e., their membrane potential is negative. but how can we measure membrane charge?

patch clamp

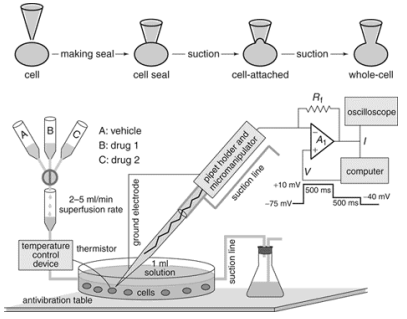

the experiment that allows the study of single or multiple ion channels is called **patch clamp**. it uses a glass **micropipette** to measure the membrane potential. the pipette can have a tip diameter of only 1um enclosing a membrane surface area or patch that contains one or just a few ion channels.

patch clamp

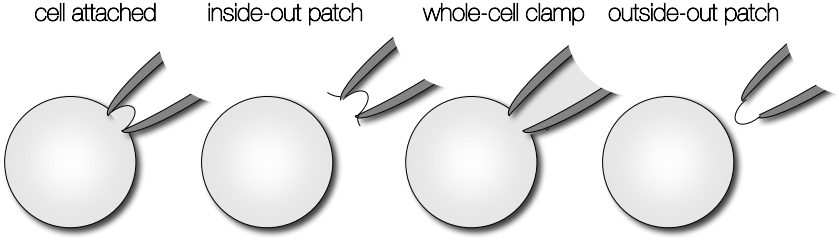

depending on the goal of the study, several variations of **patch clamp** technique can be applied. in **inside-out** and **outside-out** techniques the patch is removed from the main cell body. inside-out, outside-out, and **cell attached** techniques can be used to study the behavior of individual channels whereas **whole-cell clamp** is used to study the behavior of the entire cell.

microelectrode arrays

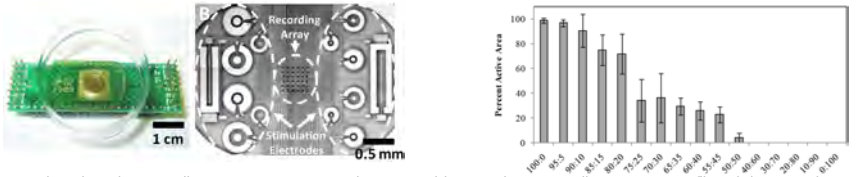

conduction in cardiomyocyte co-cultures with varying cardiomyocyte:fibroblast ratios

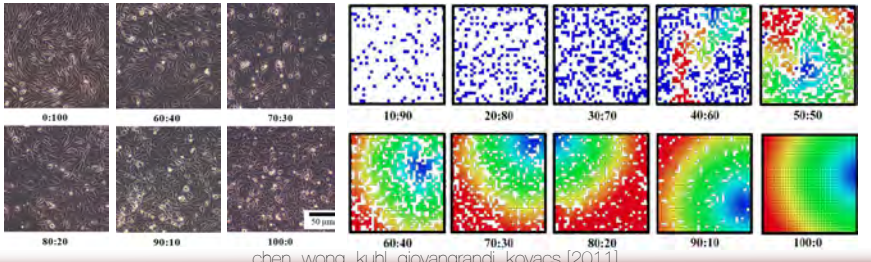

chen, wong, kuhl, giovangrandi, kovacs [2011]

membrane potential

	Na^+_{int} mM	Na^+_{ext} mM	K^+_{int} mM	K^+_{ext} mM	Cl^-_{int} mM	Cl^-_{ext} mM	resting pot. mV
nerve cell	50	437	397	20	40	556	ϕ =-65
skeletal muscle cell	13	110	138	2.5	3	90	ϕ =-99
cardiac muscle cell	10	145	135	4	25	140	ϕ =-90
red blood cell	19	155	136	5	78	112	ϕ =- 8

Table 6.2: Typical values for intracellular and extracellular concentrations of sodium (Na^+), potassium (K^+), and chloride (Cl^-) ions.

- why is there a potential difference across the cell membrane?
- what are the mechanisms that are responsible for generating, maintaining, and regulating membrane potentials?

membrane potential

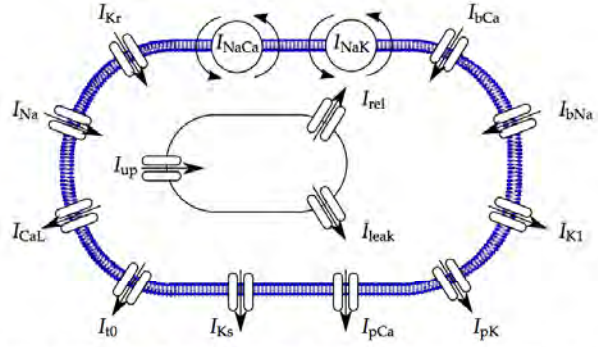

Figure 6.5: Human ventricular cardiomyocyte. In this model, the chemical state of the cardiomyocyte is characterized in terms of four ion concentrations: the free intracellular sodium, potassium, and calcium concentrations and the free calcium concentration in the sarcoplastic reticulum. Ion concentrations are controlled through 15 ionic currents,

wong, goktepe, kuhl [2010]

passive transport - ion channels

ion channels are integrated membrane proteins through which ions can diffuse through the membrane. they can be either fully open or fully closed. ionic current is dependent on both **concentration gradient** and **membrane potential**.

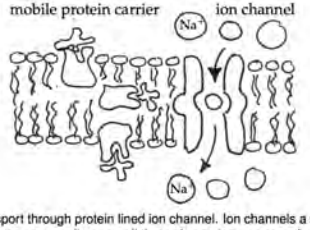

Figure 6.5: Passive transport through protein lined ion channel. Ion channels a specified for a particular class of ions and their pores are usually so small that only one ion can pass through it at a time.

- voltage-gated channels
- ligand gated channels
- mechanically gated channels
- light gated channels

active transport - ion pumps

active transport requires extra energy in the form of ATP. it is directed **against concentration gradients**, from low to high.

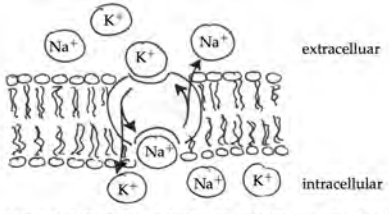

Figure 6.6: Active transport through cell membrane containing sodium/potassium pump. The Na^+/K^+ pump is the most important ion pump that consumes up to one third of the total energy requirement of a typical animal cell to actively pump cells against concentration gradients.

- example sodium potassium pump
- requires about 1/3 of all the energy of a typical animal cell

membrane potential

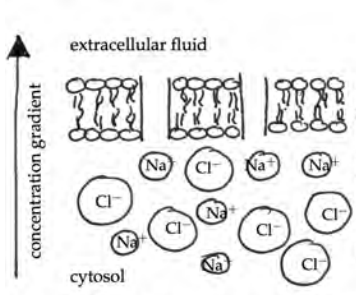

phase I electrically neutral state initially, both reservoirs contain the same ions, but at different concentrations. both sides are electrically neutral. each + ion is balanced with a - ion on each side of the membrane.

electrically neutral, but concentration gradients

membrane potential

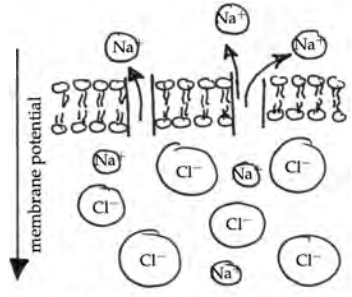

phase II selective permeability now the membrane is made permeable to sodium but not to chloride. concentration difference initiates passive transport of Na^+ along concentration gradients while Cl^- distribution remains unchanged.

equilibrated Na concentration, but electrically charged

membrane potential

phase III resting state an equilibrium state is reached when concentration-gradient driven diffusion is balanced by membrane-potential driven forces that keep ions from diffusing

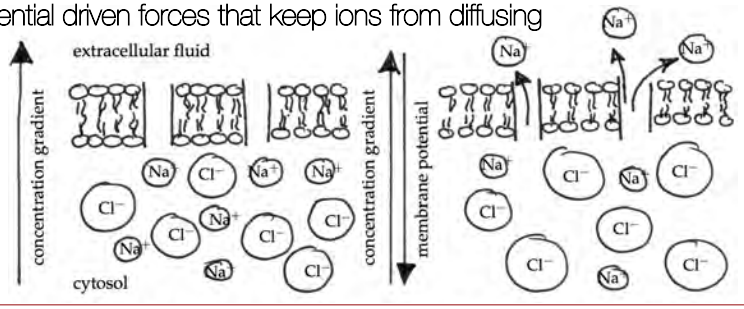

balance of concentration gradients & electric charges

membrane potential

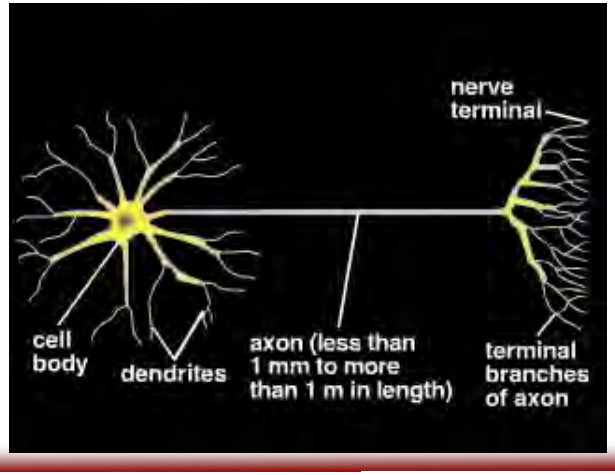

41,200,000 ions…

Let's calculate how many charged sodium ions have to move through the cell membrane of a cardiomyocyate during an action potential upstroke. This will give us an idea how much the intracellular sodium concentration changes. Assume the membrane potential during a typical upstroke increases by $\Delta\phi$=100 mV in Δt=2ms. With this information, we can determine the sodium current $I_{Na+} = c_m A \cdot \Delta\phi / \Delta t$ for a given capacitance per area c_m multiplied by a particular cell surface area A. Assume the capacitance per area is c_m=0.02 F/m^2=0.02 C/[V m^2]. Let's approximate cardiomyocytes to have a shape of a cylinder with radius $r = 5\mu$m and length $L = 100\mu$m. Their surface area then is $A = 2\pi \cdot r^2 + 2\pi \cdot r \cdot L = 2\pi \cdot [5 \cdot 10^{-6}]^2\text{m}^2 + 2\pi \cdot [5 \cdot 10^{-6}] \cdot [100 \cdot 10^{-6}]\text{m}^2 = 3.299\,10^{-9}\text{m}^2$. Solving $I_{Na+} = c_m A \cdot \Delta\phi / \Delta t$ yields a sodium current of $I_{Na+} = [0.02\text{C/V m}^2] \cdot [3.299 \cdot 10^{-9}\text{m}^2] \cdot [0.1\text{V}] / [0.002\text{s}] = 3.299 \cdot 10^{-9}$ C/s. Here C represents the unit Coulomb. Next, we need to calculate the number of ions n that are required to generate this charge. For sodium, every ion has one elementary charge, and one Coulomb then corresponds to 1C= $6.24 \cdot 10^{18}$ ions, thus $n = I_{Na+} \cdot \Delta t \cdot 6.24 \cdot 10^{18}$ ions / C. So in our case, $n = [3.299 \cdot 10^{-9}\text{ C/s}] \cdot [0.002\text{s}] \cdot [6.24 \cdot 10^{18}\text{ ions / C}] = 4.12 \cdot 10^7$. This means that it requires the movement of 41.2 million sodium ions across the membrane to change the membrane potential of cardiomyocyte by 100 mV in 2 ms!

… change the concentration by < 0.5%

$[6.24 \cdot 10^{18}\text{ ions / C}] = 4.12 \cdot 10^7$. This means that it requires the movement of 41.2 million sodium ions across the membrane to change the membrane potential of cardiomyocyte by 100 mV in 2 ms! Okay, but now, what does this mean for the intracellular sodium concentration? Assume the intracellular sodium concentration in cardiomyocytes at rest is about C_{Na+}=15 mM. Remember that 1 M = 1 mol/L and that 1 mol corresponds to $6.022 \cdot 10^{23}$ ions. So $4.21 \cdot 10^7$ ions would correspond to a change in concentration of $\Delta C_{Na+} = n / [V \cdot 6.022 \cdot 10^{23}\text{ions / mol}]$. With the assumed radius of $r = 5\mu$m and length $L = 100\mu$m, the cardiomyocyte volume is $V = \pi \cdot r^2 \cdot L = \pi \cdot [5 \cdot 10^{-6}]^2 \cdot [100 \cdot 10^{-6}]\text{m}^3 = 7.8540 \cdot 10^{-15}\text{m}^3 = 7.8540 \cdot 10^{-12}$ L. The change in concentration then results as $\Delta C_{Na+} = [4.12 \cdot 10^7\text{ ions}] / [7.85 \cdot 10^{-12}\text{L}] / [6.022 \cdot 10^{23}\text{ions / mol}] = 7.77 \cdot 10^{-5}$ mol / L = 0.0777mM. So, what is the relative change of sodium ions in the cell? $\Delta C_{Na+} / C_{Na+} = 0.0777\text{mM} / 15\text{mM} = 0.0052 = 0.52\%$. Since the normal inside concentration of sodium is approximately 15 mM, an amount of 0.077mM entering the cell during the action potential upstroke only corresponds to 0.52 % extra sodium ions. That's seems like nothing!! In summary, approximately 40 million sodium ions must cross the membrane to move the membrane potential by 100 mV in 2 ms, and that this constitutes only some 0.5% of the sodium already present in the cell.

action potentials in different cell types

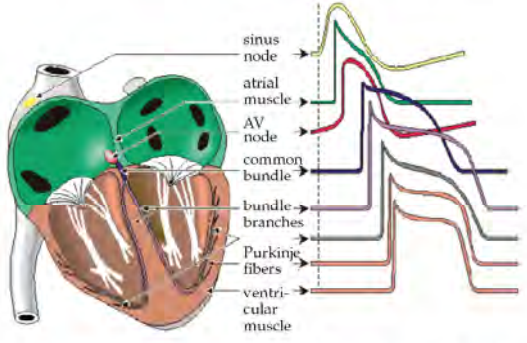

Figure 6.9: Electrophysiology of the heart: Characteristic action potentials and activation delay for various different cell types in the heart, adopted from [15].

fitzhugh-nagumo model

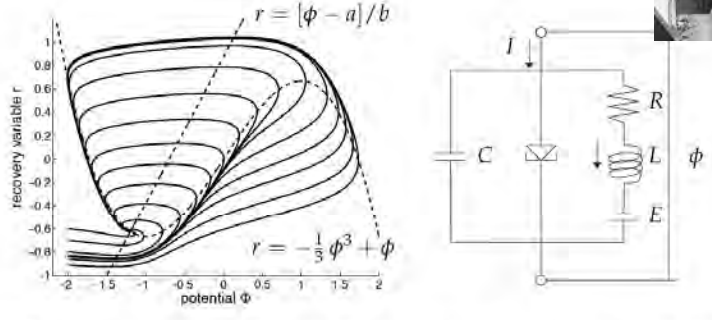

Figure 6.10: Phase portrait of classical FitzHugh-Nagumo model with a=0.7, b=0.8, c=3, left. Trajectories for distinct initial values of potential ϕ and recovery variable r converge to steady state. Dashed lines denote nullclines with $r = -\frac{1}{3}\phi^3 + \phi$ for $\dot{\phi} = 0$ and $r = [\phi - a]/b$ for $\dot{r} = 0$. Circuit diagram of corresponding tunnel-diode nerve model, right.

fitzhugh-nagumo model

- oscillator with quadratic damping coefficient

$$\ddot{\phi} + k\dot{\phi} + \phi = 0 \qquad k = c\left[\phi^2 - 1\right]$$

- nonlinear second order equation

$$\ddot{\phi} + c\left[\phi^2 - 1\right]\dot{\phi} + \phi = 0$$

- lienard's transformation

$$r = -\tfrac{1}{c}\dot{\phi} - \tfrac{1}{3}\phi^3 + \phi \qquad \dot{r} = -\tfrac{1}{c}\ddot{\phi} - \left[\phi^2 - 1\right]\dot{\phi}$$

- two first order equations

$$\dot{\phi} = c\left[-\tfrac{1}{3}\phi^3 + \phi - r\right] \qquad \dot{r} = \tfrac{1}{c}\,\phi$$

- classical fitzhugh-nagumo model for excitable cells

$$\dot{\phi} = c\left[-\tfrac{1}{3}\phi^3 + \phi - r + I\right] \quad \dot{r} = \tfrac{1}{c}\left[\phi - b\,r - a\right]$$

fitzhugh-nagumo model

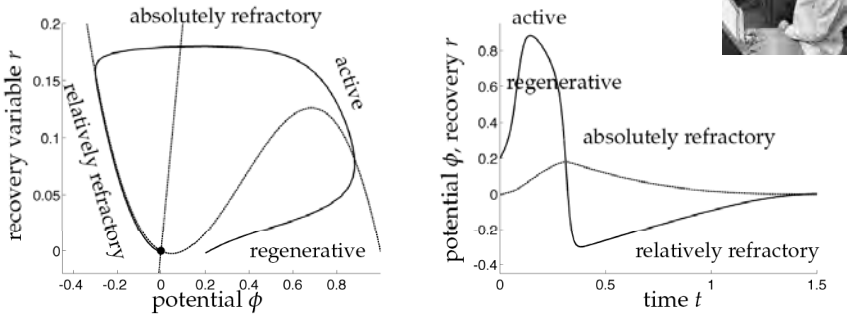

Figure 6.11: Four phases of the action potential: Regenerative phase, active phase, absolutely refractory phase, and relatively refractory phase. Simulations are based on the classical FitzHugh-Nagumo model Dashed lines in the phase portrait illustrate the nullclines, the dot at their intersection corresponds to the resting state, left. In the physiological state diagram, solid lines indicate the temporal evolution of the membrane potential ϕ and dashed lines correspond to the recovery variable r, right.

four phases of excitation

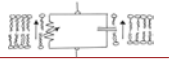

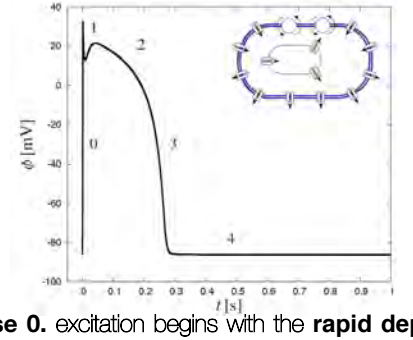

regenerative phase 0. excitation begins with the **rapid depolarization** of the cell characterized through a **fast upstroke** of the membrane potential. the depolarization opens both sodium and potassium channels initiating an outward potassium current and an inward sodium current. for sufficiently large stimuli, a positive feedback is generated. more and more **sodium channels** open. the membrane potential increases rapidly.

four phases of excitation

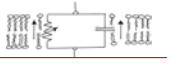

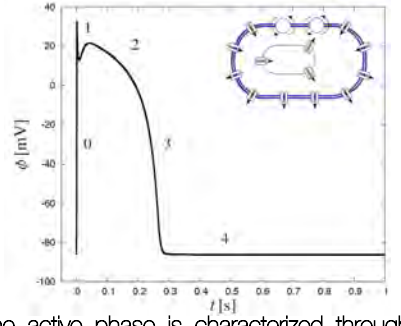

active phase 1. the active phase is characterized through a **high and almost constant membrane potential**. sodium permeability is maximized but decreases as more and more sodium channels tend to close again. also, potassium channels now begin to open. this marks the end of the active phase.

four phases of excitation

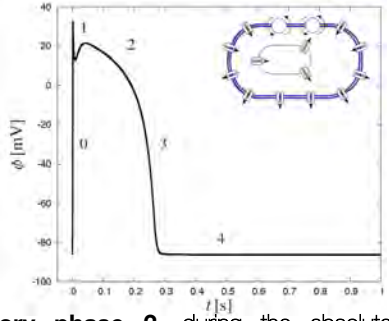

absolutely refractory phase 2. during the absolutely refractory phase the **membrane potential decreases smoothly**. some cell types tend to hyperpolarize, they initially overshoot the resting state. action potentials cannot follow one another immediately since the ion channels need to return to their resting state. during the **absolutely refractory period** the cell is unable to generate a new action potential.

four phases of excitation

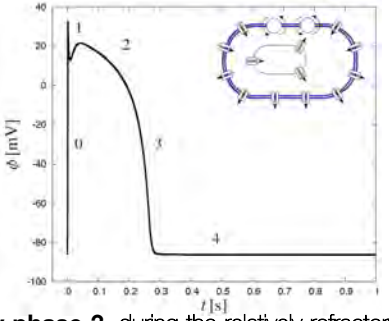

relatively refractory phase 3. during the relatively refractory phase the **cell slowly returns to the resting state**. the ion channels also gradually go back to their initial state. a new action potential can be generated during this phase, however, the required stimulus might be significantly larger than if the cell was already at rest.

action potentials in different cell types

animal	cell type	resting potential [mV]	potential increase [mV]	potential duration [ms]	conductivity [m/s]
squid (loligo)	giant axon	-60	120	0.75	35
earthworm (lumbricus)	median giant fiber	-70	100	1.00	30
cockroach (periplaneta)	giant fiber	-70	80–104	0.40	10
frog (rana)	sciatic nerve axon	-60 – -80	110–130	1.00	7-30

Table 6.2: Typical value of resting potential, action potential increase, action potential duration, and conduction speed for action potentials of different cell types.

motivation - nerve cells

bonhoeffer-van der pol oscillator

$$\ddot{\phi} + k\,\dot{\phi} + \phi = 0 \qquad k = c[\,\phi^2 - 1\,]$$

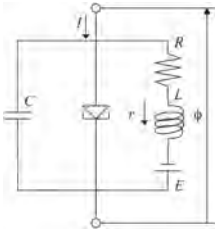

fitzhugh-nagumo equation

$$\begin{aligned} \dot{\phi} &= f^{\phi}(\phi, r) + \operatorname{div}(\boldsymbol{q}) && \text{potential} \\ \dot{r} &= f^{r}(\phi, r) && \text{repolarization} \end{aligned}$$

$$\boldsymbol{q} = [\,d^{\text{iso}}\boldsymbol{I} + d^{\text{ani}}\boldsymbol{n} \otimes \boldsymbol{n}\,] \cdot \nabla\phi$$

van der pol [1926], hodgkin & huxley [1952], fitzhugh [1961], nagumo et al. [1962]

oscillatory pacemaker cells vs stable muscle cells

$$f^{\phi} = -c\,\phi\,[\phi - a][\phi - 1] - c\,r$$
$$f^{r} = \phi - b\,r + a$$

$$f^{\phi} = -c\,\phi\,[\phi - a][\phi - 1] - r\phi$$
$$f^{r} = [\gamma + \tfrac{\mu_1\, r}{\mu_2 + \phi}][-r - c\,\phi[\phi - b - 1]]$$

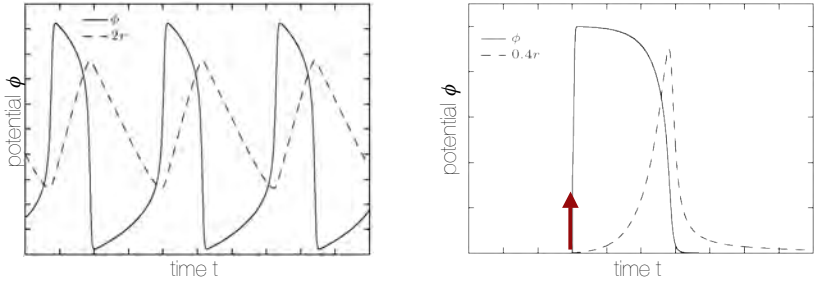

hodgkin & huxley [1952], fitzhugh [1961], noble [1962], beeler & reuter [1977], luo & rudy [1991]
aliev & panfilov [1996], rogers & mc culloch [1994], nash & panfilov [2004]

healthy tissue - in vitro vs in silico

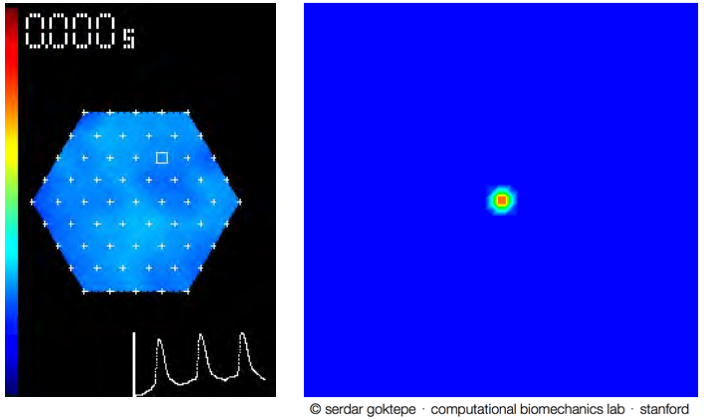

courtesy of kit parker, disease biophysics group, harvard university

fibrillating tissue - in vitro vs in silico

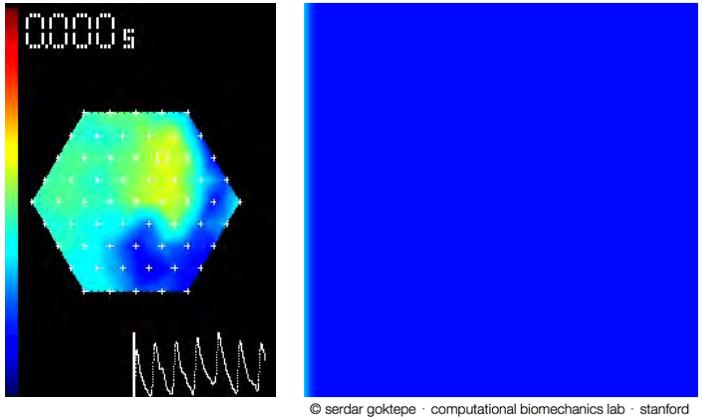

courtesy of kit parker, disease biophysics group, harvard university

excitation of a mouse heart

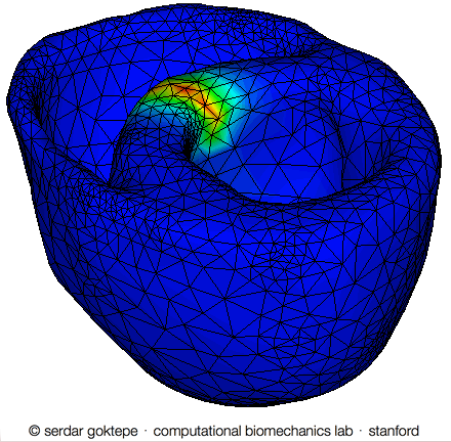

re-entry and ventricular fibrillation - *in silico* prediction

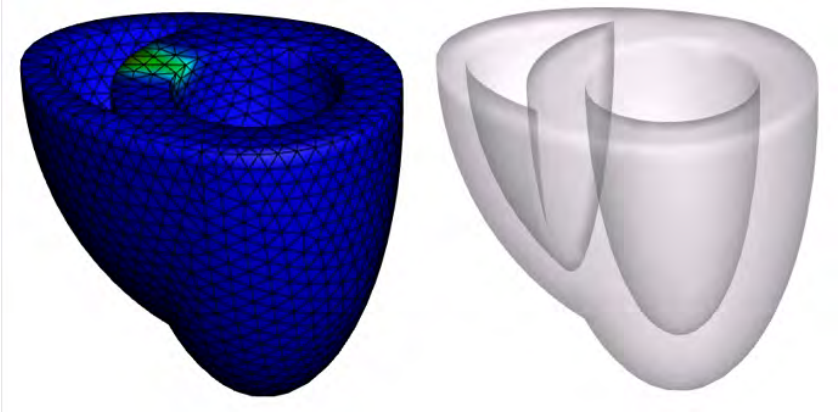

göktepe, wong, kuhl [2010]

what can we do about it?

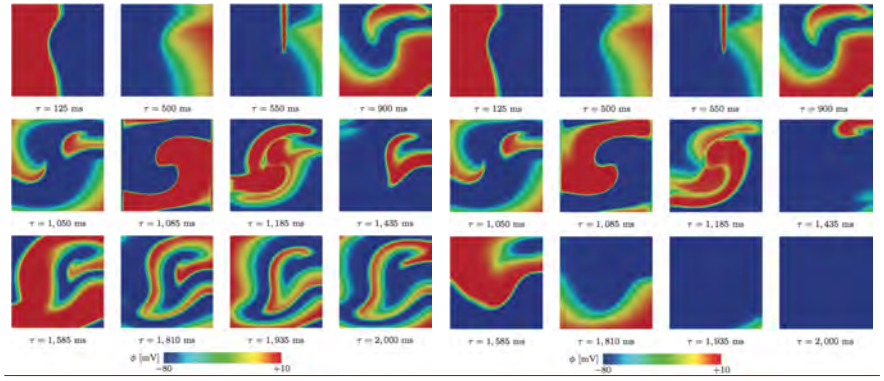

unsuccessful vs successful defibrillation

dal, göktepe, kaliske, kuhl [2010]

excitation of a human heart - mri

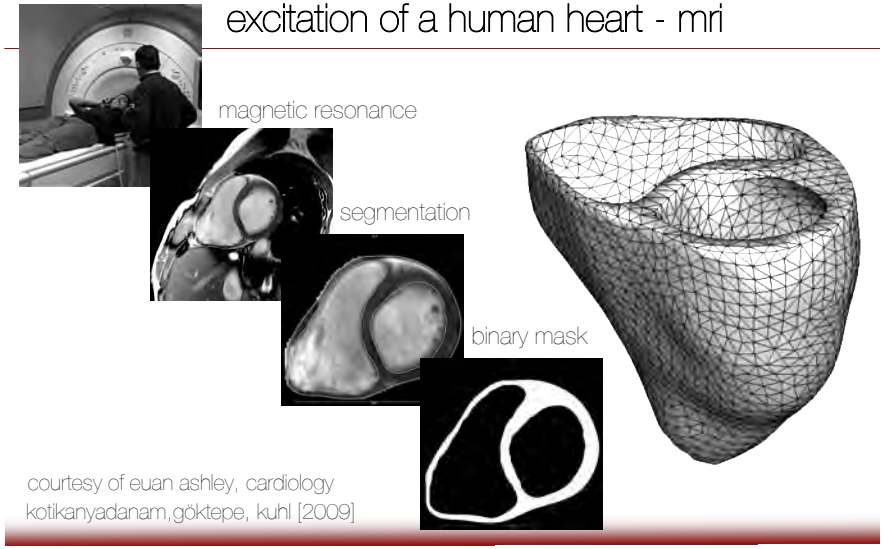

courtesy of euan ashley, cardiology
kotikanyadanam,göktepe, kuhl [2009]

excitation of a human heart - ekg

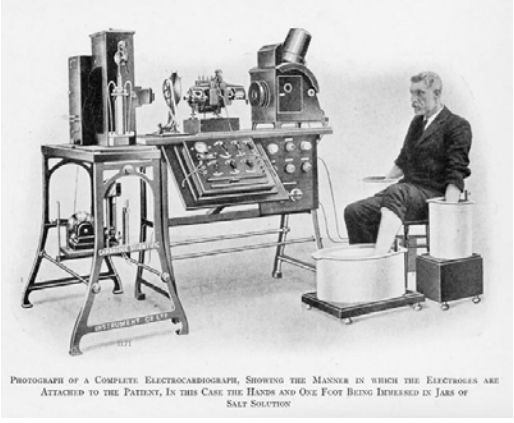

PHOTOGRAPH OF A COMPLETE ELECTROCARDIOGRAPH, SHOWING THE MANNER IN WHICH THE ELECTRODES ARE ATTACHED TO THE PATIENT, IN THIS CASE THE HANDS AND ONE FOOT BEING IMMERSED IN JARS OF SALT SOLUTION

1st ekg willem einthoven [1903], nobel prize in medicine [1924]

excitation of a human heart - ekg

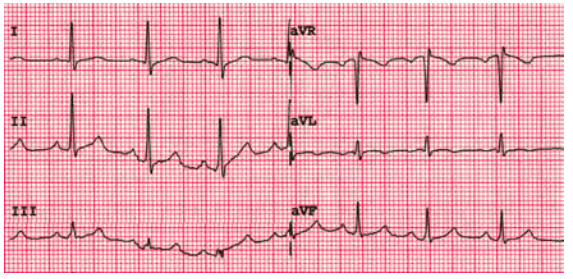

- P wave - depolarization of the atria
- QRS complex - depolarization of the ventricles
- T wave - repolarization of the ventricles

courtesy of oscar abilez, bioengineering / vascular surgery, stanford

excitation of a human heart - heart vector

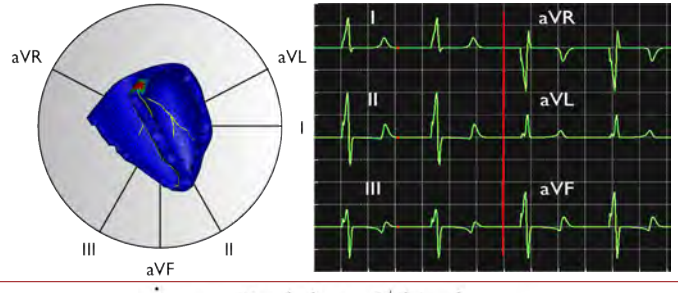

$$\dot{\phi} = \operatorname{div}(\boldsymbol{q}) + f^{\phi}(\phi, r)$$

$$\boldsymbol{q} = [\, d^{\text{iso}}\boldsymbol{I} + d^{\text{ani}}\boldsymbol{n} \otimes \boldsymbol{n}\,] \cdot \nabla\phi$$

$$\boldsymbol{q}^{\text{hrt}} = \int_{\text{dV}} \boldsymbol{q}\, \text{dV}$$

kotikanyadanam,göktepe, kuhl [2009]

excitation of a human heart - computational model

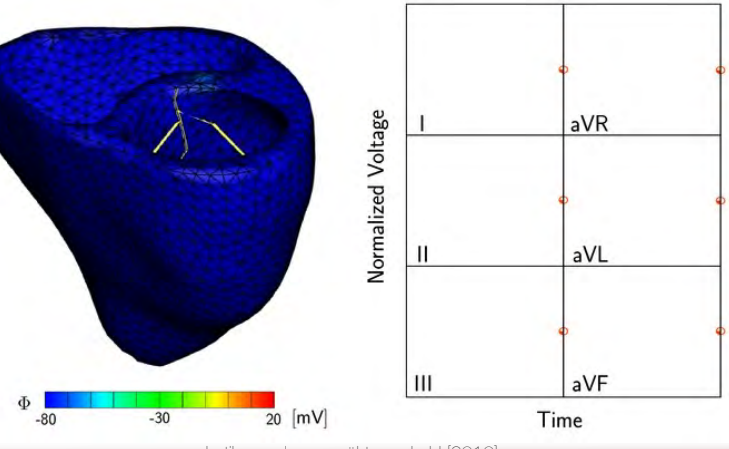

kotikanyadanam,göktepe, kuhl [2010]

excitation of a human heart

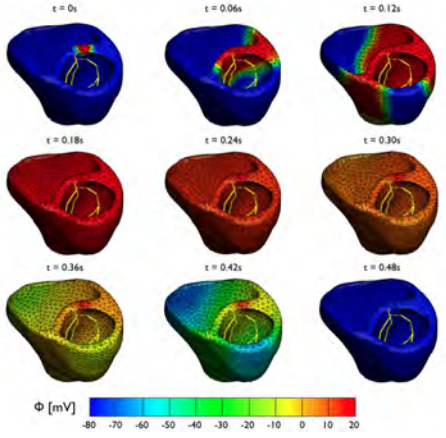

kotikanyadanam,göktepe, kuhl [2010]

electrochemical model of a heart cell

ten tuscher, noble, noble, panfilov model

$$\dot{\phi} = \operatorname{div} \boldsymbol{q}(\phi) + f^{\phi}(\phi, g_{\text{gate}}, c_{\text{ion}}) \qquad \boldsymbol{q} = [\, d^{\text{iso}} \boldsymbol{I} + d^{\text{ani}} \boldsymbol{n} \otimes \boldsymbol{n} \,] \cdot \nabla \phi$$

action potential evolution as a result of ionic currents

$$f^{\phi} = -[\, I_{\text{Na}} + I_{\text{bNa}} + I_{\text{NaK}} + I_{\text{NaCa}} + I_{\text{K1}} + I_{\text{Kr}} + I_{\text{Ks}} + I_{\text{pK}} + I_{\text{t0}} + I_{\text{CaL}} + I_{\text{bCa}} + I_{\text{pCa}} \,]$$

ionic currents

$$I_{\text{crt}} = I_{\text{crt}}(\phi, g_{\text{gate}}, c_{\text{ion}})$$

gating variables

$$g_{\text{gate}} = g^{n}_{\text{gate}} + \frac{1}{\tau_{\text{gate}}(\phi)} [\, g^{\infty}_{\text{gate}}(\phi) - g_{\text{gate}} \,] \, \Delta t$$

ion concentrations

$$\dot{c}_{\text{ion}} = \dot{c}_{\text{ion}}(\phi, g_{\text{gate}}, c_{\text{ion}})$$

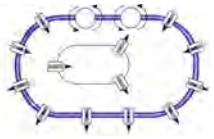

beeler, reuter [1977], luo, rudy [1991], ten tuscher, noble, noble, panfilov [2004], wong, göktepe, kuhl [2010]

human ventricular cardiomyocyte

	sodium related	potassium related	calcium related	calcium^{sr} related
concentrations	$c_{\text{Na0}} = 140$ mM	$c_{\text{K0}} = 5.4$ mM	$c_{\text{Ca0}} = 2$ mM	-
maximum currents	$I^{\text{max}}_{\text{NaCa}} = 1000$ pA/pF $I^{\text{max}}_{\text{NaK}} = 1.362$ pA/pF	$I^{\text{max}}_{\text{NaK}} = 1.362$ pA/pF	$I^{\text{max}}_{\text{NaCa}} = 1000$ pA/pF $I^{\text{max}}_{\text{leak}} = 0.08$ mm/s $I^{\text{max}}_{\text{up}} = 0.425$ mM/s $I^{\text{max}}_{\text{rel}} = 8.232$ mM/s	$I^{\text{max}}_{\text{leak}} = 0.08$ mm/s $I^{\text{max}}_{\text{up}} = 0.425$ mM/s $I^{\text{max}}_{\text{rel}} = 8.232$ mM/s
maximum conductances	$C^{\text{max}}_{\text{Na}} = 14.838$ nS/pF $C^{\text{max}}_{\text{bNa}} = 0.00029$ nS/pF	$C^{\text{max}}_{\text{K1}} = 5.405$ nS/pF $C^{\text{max}}_{\text{Kr}} = 0.0096$ nS/pF $C^{\text{max}}_{\text{Ks,epi}} = 0.245$ nS/pF $C^{\text{max}}_{\text{Ks,endo}} = 0.062$ nS/pF $C^{\text{max}}_{\text{pK}} = 0.0146$ nS/pF $C^{\text{max}}_{\text{t0}} = 0.294$ nS/pF	$C^{\text{max}}_{\text{CaL}} = 0.175\text{mm}^3/[\mu\text{Fs}]$ $C^{\text{max}}_{\text{bCa}} = 0.000592$ nS/pF $C^{\text{max}}_{\text{pCa}} = 0.025$ nS/pF	
half saturation constants	$c_{\text{CaNa}} = 1.38$ mM $c_{\text{NaCa}} = 87.50$ mM $c_{\text{KNa}} = 1.00$ mM $c_{\text{NaK}} = 40.00$ mM	$c_{\text{KNa}} = 1.00$ mM $c_{\text{NaK}} = 40.00$ mM	$c_{\text{CaNa}} = 1.38$ mM $c_{\text{NaCa}} = 87.50$ mM $c_{\text{pCa}} = 0.0005$ mM $c_{\text{up}} = 0.00025$ mM $c_{\text{rel}} = 0.25$ mM $c_{\text{bsf}} = 0.001$ mM	$c_{\text{up}} = 0.00025$ mM $c_{\text{rel}} = 0.25$ mM $c^{\text{sr}}_{\text{bsf}} = 0.3$ mM
other parameters	$k^{\text{sat}} = 0.10$ $\gamma_{\text{NaCa}} = 2.50$ $\gamma = 0.35$	$p_{\text{KNa}} = 0.03$	$\gamma_{\text{rel}} = 2$ $c_{\text{tot}} = 0.15$ mM	$\gamma_{\text{rel}} = 2$ $c^{\text{sr}}_{\text{tot}} = 10$ mM
gas constant $R = 8.3143\,\text{J K}^{-1}\,\text{mol}^{-1}$	temperature $T = 310$ K	cytoplasmic volume $V = 16404\mu m^3$		
Faraday constant $F = 96.4867$ C/mmol	cell capacitance $C = 2\,\mu\text{F/cm}^2$	sarcoplastic reticulum volume $V^{\text{sr}} = 1094\mu m^3$		

beeler, reuter [1977], luo, rudy [1991], ten tuscher et al. [2004], wong,göktepe, kuhl [2010]

electrochemical model - 13 gating variables

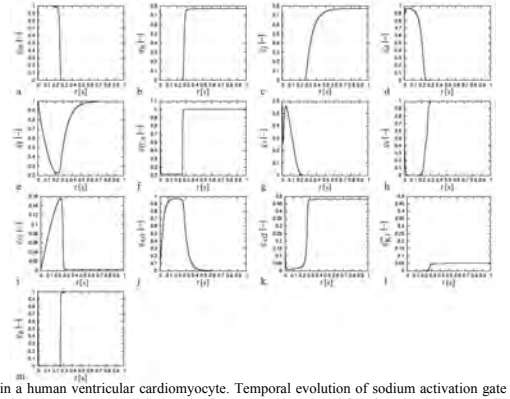

Figure 3. Electrochemistry in a human ventricular cardiomyocyte. Temporal evolution of sodium activation gate g_m, fast sodium inactivation gate g_h, slow sodium inactivation gate g_j, L-type calcium activation gate g_d, L-type calcium inactivation gate g_f, intracellular calcium dependent calcium inactivation gate g_{fCa}, transient outward activation gate g_r, transient outward inactivation gate g_s, slow delayed rectifier gate g_{xs}, rapid delayed rectifier activation gate g_{xr1}, rapid delayed rectifier inactivation gate g_{mxr2}, inward recrification factor $g_{K1\infty}$, and calcium-dependent inactivation gate g_g.

electrochemical model - 15 ionic currents

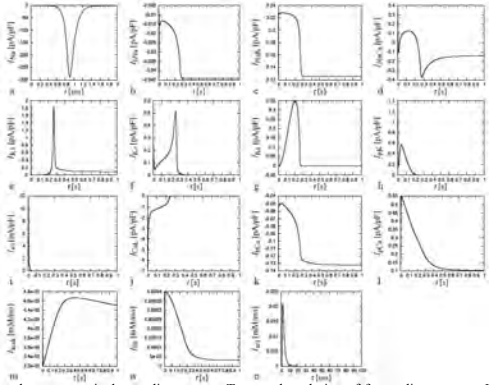

Figure 4. Electrochemistry in a human ventricular cardiomyocyte. Temporal evolution of fast sodium current I_{Na}, background sodium current I_{bNa}, sodium potassium pump current I_{NaK}, sodium calcium exchanger current I_{NaCa}, inward rectifier current I_{K1}, rapid delayed rectifier current I_{Kr}, slow delayed rectifier current I_{Ks}, plateau potassium current I_{pK}, transient outward current I_{t0}, L-type calcium current I_{CaL}, background calcium current I_{bCa}, plateau calcium current I_{pCa}, leakage current I_{leak}, sarcoplastic reticulum uptake current I_{up}, and sarcoplastic reticulum release current I_{rel}.

electrochemical model - 4 ion concentrations

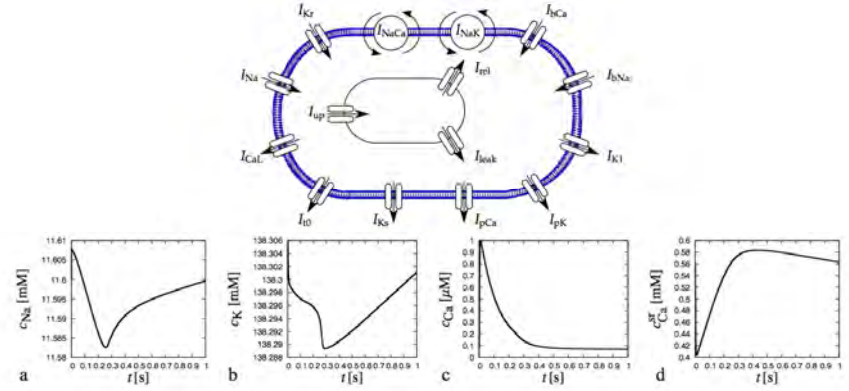

Figure 6: Chemo-electrical coupling in a human ventricular cardiomyocyte. Temporal evolution of intracellular sodium concentration c_{Na}, potassium concentration c_K, calcium concentration c_{Ca}, and calcium concentration in the sarcomplastic reticulum c_{Ca}^{SR}.

electrochemical model of the heart

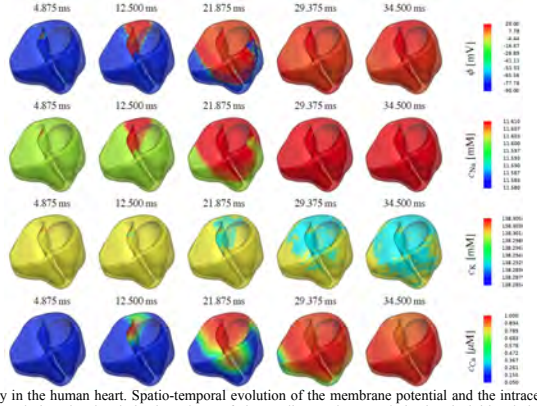

Figure 6. Electrochemistry in the human heart. Spatio-temporal evolution of the membrane potential and the intracellular sodium, potassium, and calcium concentrations during the depolarization phase of the cardiac cycle. Depolarization is initiated through an increase in the intracellular sodium concentration which reflects itself in the rapid depolarization of the cell characterized through an increase in the transmembrane potential from -86mV to +20mV.

wong, goktepe, kuhl [2010]

electrochemical model of the heart

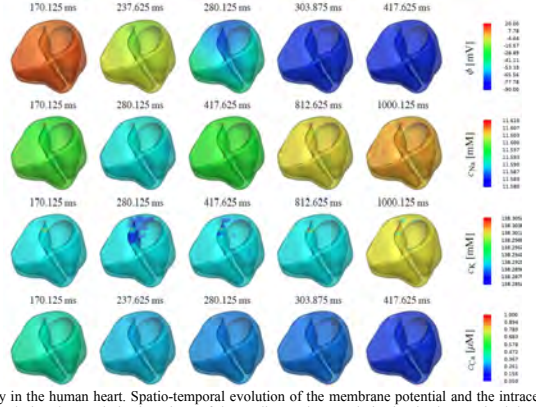

Figure 7. Electrochemistry in the human heart. Spatio-temporal evolution of the membrane potential and the intracellular sodium, potassium, and calcium concentrations during the repolarization phase of the cardiac cycle. Repolarization is characterized through a smooth decrease in the transmembrane potential from its excited value of +20mV back to its resting value of -86mV. At the same time, the three ion concentrations return to their resting values.

wong, goktepe, kuhl [2010]

electro-mechanical coupling

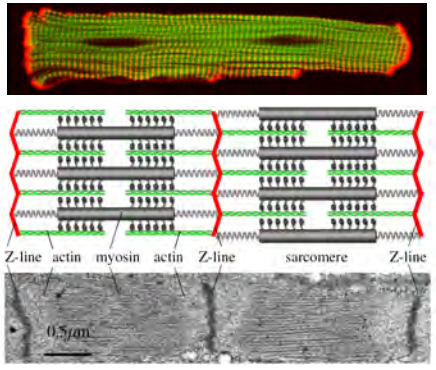

- **electrical** excitation induces **mechanical** contraction
- **mechanical** contraction affects stretch-induced **ion channels**

aliev & panfilov [1996], rogers & mc culloch [1994], tentusscher & panfilov [2008]

actin-myosin interaction for muscle contraction

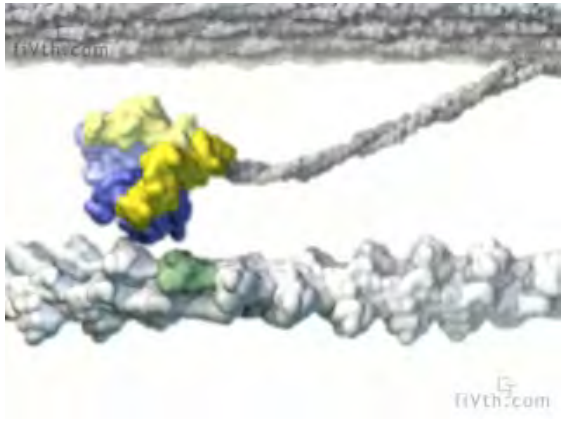

actin-myosin interaction for muscle contraction

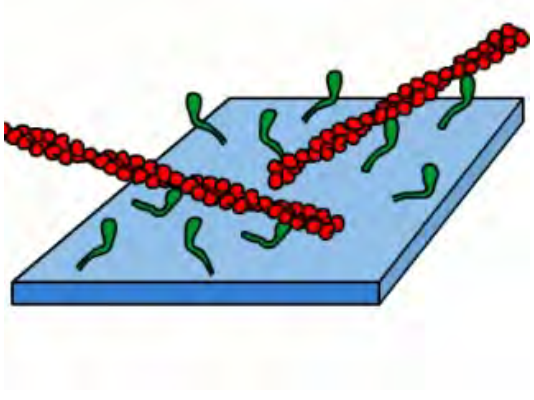

actin-myosin interaction for muscle contraction

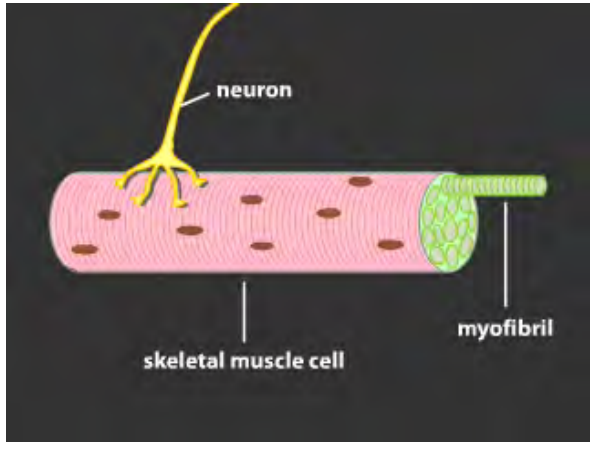

electro-mechanical coupling

- primary field variables
  $\phi, \boldsymbol{\varphi}$
- differential equations

$$\dot{\phi} = J \operatorname{div}(J^{-1}\boldsymbol{q}) + f^{\phi}$$
$$\mathbf{0} = J \operatorname{div}(J^{-1}\boldsymbol{\tau}) + \boldsymbol{f}^{\varphi}$$

- constitutive coupling

$$\boldsymbol{q} = \boldsymbol{q}\ (\nabla_X \boldsymbol{\varphi}, \nabla_x \phi)$$
$$f^{\phi} = f^{\phi}\ (\nabla_X \boldsymbol{\varphi}, \phi)$$
$$\boldsymbol{\tau} = \boldsymbol{\tau}^{\text{pas}}(\nabla_X \boldsymbol{\varphi}) + \tau^{\text{act}}(\nabla_X \boldsymbol{\varphi}, \phi)\, \boldsymbol{n}^{\text{myo}} \otimes \boldsymbol{n}^{\text{myo}}$$

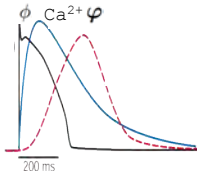

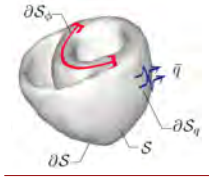

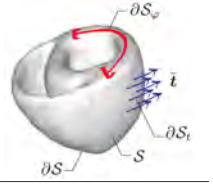

fully coupled monolithic fe model

göktepe & kuhl [2010]

mechanically induced excitation

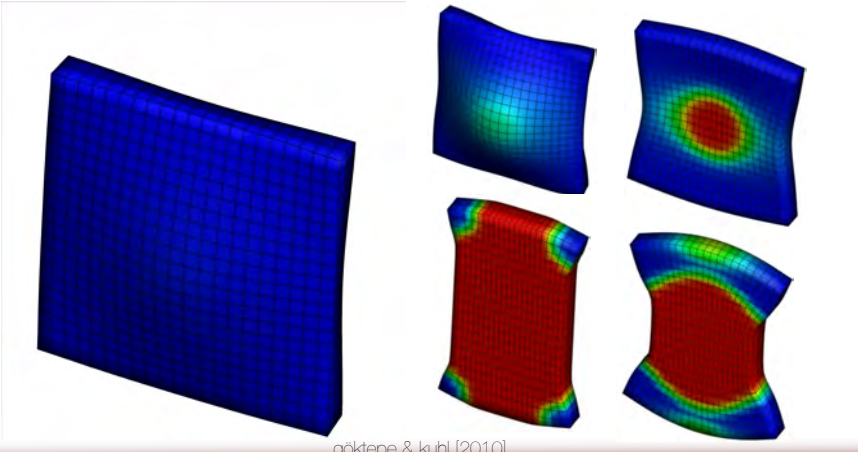

göktepe & kuhl [2010]

electrically induced contraction

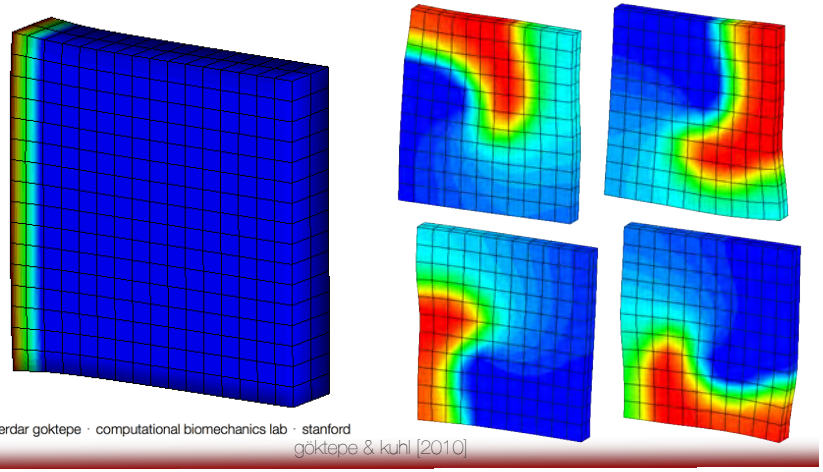

göktepe & kuhl [2010]

generic bi-ventricular heart model

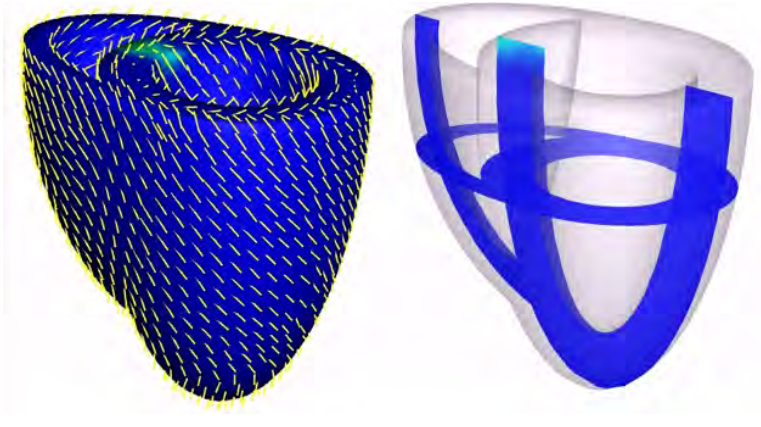

göktepe & kuhl [2010]

generic bi-ventricular heart model

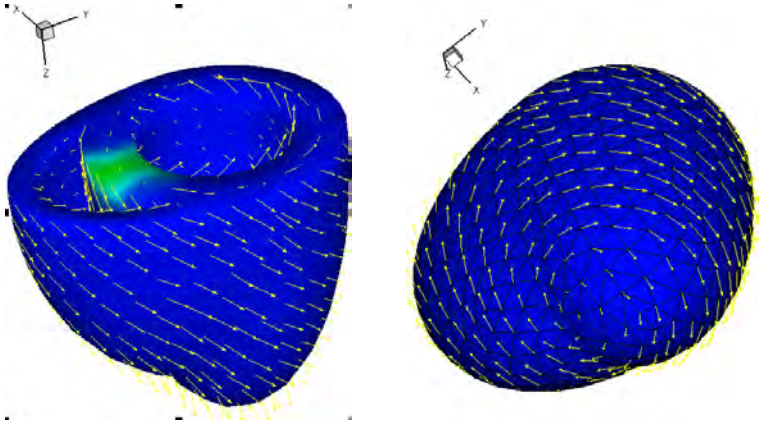

göktepe & kuhl [2010]

patient-specific heart

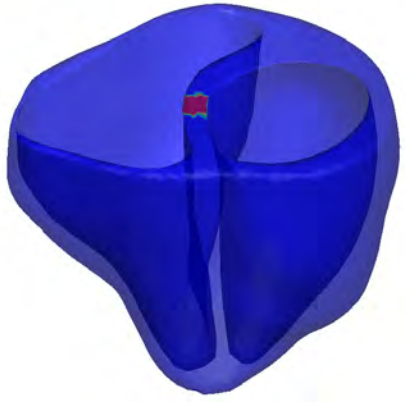

wong, göktepe & kuhl [2012]

pressure volume loops

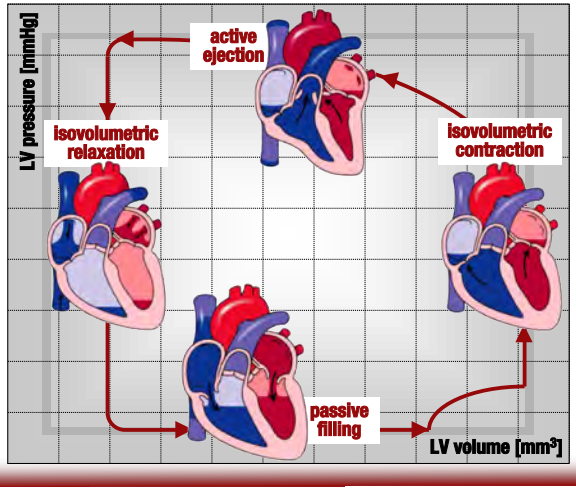

pressure volume loops

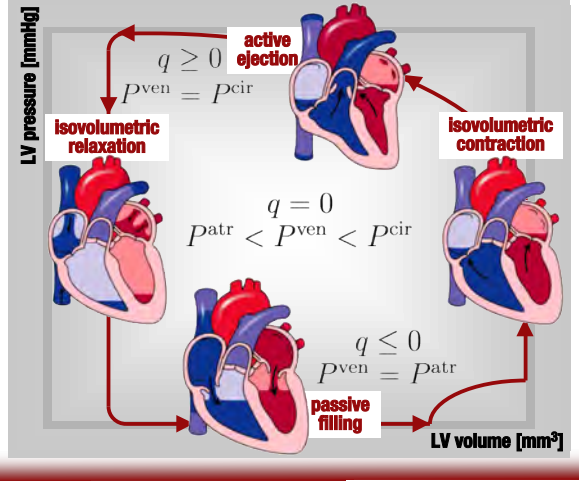

$q = -\dot{V}(t)$

pressure volume relation / signorini contact problem

regularize → invert →

$q = q\,(P^{\text{ven}}, P^{\text{cir}}, P^{\text{atr}})$ $\quad q = q\,(P^{\text{ven}}, P^{\text{cir}}, P^{\text{atr}})$ $\quad P^{\text{ven}} = P^{\text{ven}}(q, P^{\text{cir}}, P^{\text{atr}})$

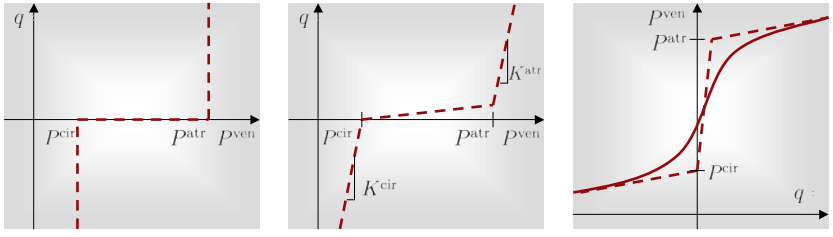

smooth →

$$P^{\text{ven}} = \epsilon_0 + [\epsilon_\infty - \epsilon_0]\exp(-\exp(\xi\, q)) \qquad q = -\dot{V}(t)$$

$$\epsilon_0 = \frac{1}{K^{\text{atr}}}\, q + P^{\text{atr}} \qquad \epsilon_\infty = \frac{1}{K^{\text{cir}}}\, q + P^{\text{cir}}$$

pressure volume loop in healthy and infarcted heart

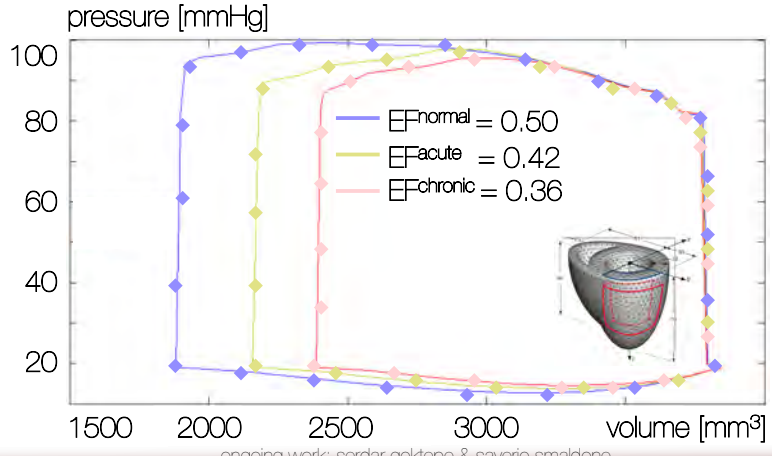

ongoing work: serdar goktepe & saverio smaldone